Separation Science and Technology
Publication details, including instructions for authors and subscription information:
http://www.informaworld.com/smpp/title~content=t713708471

Phenol Removal by Supported Liquid Membranes

F. F. Zha[a]; A. G. Fane[a]; C. J. D. Fell[a]
[a] UNESCO CENTRE FOR MEMBRANE SCIENCE AND TECHNOLOGY, UNIVERSITY OF NEW SOUTH WALES, SYDNEY, AUSTRALIA

To cite this Article Zha, F. F. , Fane, A. G. and Fell, C. J. D.(1994) 'Phenol Removal by Supported Liquid Membranes', Separation Science and Technology, 29: 17, 2317 — 2343
To link to this Article: DOI: 10.1080/01496399408003181
URL: http://dx.doi.org/10.1080/01496399408003181

SEPARATION SCIENCE AND TECHNOLOGY, **29**(17), pp. 2317–2343, 1994

Phenol Removal by Supported Liquid Membranes

F. F. ZHA, A. G. FANE,* and C. J. D. FELL
UNESCO CENTRE FOR MEMBRANE SCIENCE AND TECHNOLOGY
UNIVERSITY OF NEW SOUTH WALES
SYDNEY 2052, AUSTRALIA

ABSTRACT

This paper examines the application of the supported liquid membrane (SLM) to phenol removal. *n*-Decanol was proven to be a suitable membrane liquid. The phenol transfer kinetics through the SLMs is quantitatively estimated according to models based on the resistance-in-series concept. The models can be modified to describe the performance of decayed SLMs and thereby provide insight into the effect of membrane liquid loss and penetration of aqueous solutions on the phenol flux. An experimental method is described for the measurement of mass transfer coefficients in the bulk phases using the well-characterized Anopore membrane.

Key Words. Phenol removal; Liquid membranes; Modeling; Facilitated transport

INTRODUCTION

Phenol and phenolic compound wastes are produced from manufacturing processes such as petroleum refining, processing or manufacturing of phenol and phenolic resins, creosoting, and coal processing. Phenol concentrations in aqueous effluents from such processes range from hundred ppm to several percent. Because phenols are toxic, their disposal is highly restricted, and typically the discharge of phenolic compounds (not including pentachlorophenol) to sewers should be controlled below

* To whom correspondence should be addressed.

10 ppm. On the other hand, phenol is a valuable chemical. Therefore, recovery of phenols from phenolic effluents can achieve the dual objective of removing unwanted phenols from waste streams and obtaining valuable phenolic compounds.

There are two types of process for treating phenolic waste effluent: degradation methods and recovery methods. Chemical degradation and biological oxidation belong to the former. In degradation methods, phenols are converted into substances that are nontoxic and satisfactory for release to the environment. The main disadvantage of degradation methods is the high cost because of the large consumption of chemicals (as in chemical degradation) or major investment in equipment (as in biological treatment). The conversion of phenol into other substances means another costly loss of a valuable material. Therefore, these processes are only used for the treatment of waste phenolic streams at low concentration or in mixtures, and often as the last treatment stage.

The recovery methods commonly used in industry are adsorption, solvent extraction, and membrane technology. In a recovery process, phenols are reclaimed for recycle or as products. Solvent extraction is usually the preferred method to adsorption in the removal and recovery of phenol (1). It is desirable in solvent extraction that the solvent has a high distribution coefficient and a low solubility in water. However, these are to some extent always contradictory. The solvents with high distribution coefficients are polar organics, such as ketones, esters, and alcohols. These solvents are usually more soluble and more expensive than nonpolar hydrocarbons. Therefore, loss of solvent is usually serious (2).

Membrane technology promises interesting alternatives to the conventional methods for phenol removal and recovery. The membrane processes investigated for phenol recovery are reverse osmosis (3), ultrafiltration (4), pervaporation (5), and liquid membranes (6, 7). Among the various membrane separation technologies, supported liquid membranes (SLMs) show a most promising capability for phenol recovery. A significant advantage of SLMs is their ability to achieve high selectivity and concentrating solutes at the same time.

SLMs utilize microporous solid membranes as a support, and the solvents are immobilized within the membrane pores. The highest surface area to volume can be obtained when hollow fiber membranes are used as a support. Urtiaga et al. (7–9) explored the application of hollow fiber SLMs to the removal of phenol from wastewater. The membrane liquids they used were kerosene, methyl isobutyl ketone (MIBK), and their mixtures. The use of kerosene as a membrane liquid produced a quite stable SLM. However, the SLM displayed a large resistance to phenol transport because of the very low distribution coefficient (8). MIBK has a larger

distribution coefficient for phenol, but its high solubility in aqueous solutions greatly shortened the lifetime of the SLM (7). Recently, the same group reported the use of a commercial extractant CYANEX 923 in kerosene as the membrane phase (10). Because CYANEX 923 has a high phenol selectivity and an extremely low solubility in aqueous solutions, loss of membrane liquid decreased and phenol flux increased. However, the attainable lifetime of SLMs was not reported.

Many factors, such as properties of the membrane liquid and the substrate, operating conditions, and stability, can influence the mass transfer performance of an SLM. In this paper a fundamental investigation of phenol removal by SLMs is made. *n*-Decanol is employed as the membrane liquid because it provides a compromise between the solvent solubility in water and the phenol distribution coefficient in the solvent. This paper also develops models of the mass transfer processes of phenol separation for both integral and partially decayed SLMs.

PHENOL TRANSPORT BEHAVIORS IN SLMs

Phenol Transport through Integral SLMs

The situation considered here is the transport of phenol through a flat-sheet SLM in batch cell operation. The resistance-in-series method is adopted to give explicit results for the process. The mass transfer rate and the total resistance can be expressed in the following way if the interfacial resistances are neglected:

$$J_A = K\left(C_f - \frac{m_s}{m_f} C_s\right) \tag{1}$$

$$\frac{1}{K} = \frac{1}{k_f} + \frac{1}{m_f k_m} + \frac{m_s}{m_f k_s} \tag{2}$$

where distribution coefficient m is defined as $m = C_{org}/C_{aq}$. If the distribution coefficient of phenol does not change significantly with the concentration in the aqueous solution, it can be deduced from Eq. (1) that phenol transport will macroscopically terminate when the concentrations of phenol in the feed and strip are equal. One way to facilitate the phenol transport process is to adopt chemical reactions in the strip side. Because phenol is a weak acid, a strong basic solution is usually used as the stripping phase. The following instantaneous irreversible chemical reaction occurs:

$$PhOH + OH^- = PhO^- + H_2O \tag{3}$$

The phenolate formed does not dissolve in the organic solvent and hence

cannot diffuse back to the feed through the SLM. Mass transfer resistance in the strip side is greatly decreased and even approaches zero if the base concentration is high enough. Therefore, phenol transfer rate is much accelerated.

A model for mass transfer with instantaneous chemical reaction is described by Grosjean and Sawistowski (11), and applied to membrane extraction by Basu et al. (12). In SLMs, two situations should be considered according to the base concentration in the strip.

(1) Chemical reaction takes place at the interface between the membrane and the stripping phase. This is the case when the stripping phase contains sufficient base. The free phenol concentration at the interface of the strip side and in the stripping solution is nearly zero ($C_s \approx 0$) and phenol exists mainly in the form of phenolate. If the interfacial reaction resistance is neglected, the total mass transfer resistance comes from the feed and the membrane phase only. The phenol transfer rate and the total resistance are simplified to

$$J_A = KC_f \tag{4}$$

$$\frac{1}{K} = \frac{1}{k_f} + \frac{1}{m_f k_m} \tag{5}$$

(2) The chemical reaction front is not at the phase interface but is located somewhere in the film of the aqueous phase. This situation occurs when the stripping phase contains insufficient base. The concentration profiles are shown in Fig. 1. The critical base concentration (C'_B), below which the reaction front moves away from the phase interface into the film of the aqueous solution, can be obtained from the stoichiometric condition at the reaction front as

$$C'_B = qKC_f/k_B \tag{6}$$

where K is the mass transfer coefficient through the feed and the membrane phase and is expressed in Eq. (5), q is the stoichiometric coefficient ($q = 1$ when caustic is used in the strip), and k_B is the transfer coefficient of the base in the stripping phase. Molar concentrations should be used in Eq. (6). The dotted lines in Fig. 1 represent the concentration profiles when the base is at the critical concentration.

Grosjean and Sawistowski (11) recommended two correlations for the determination of individual mass transfer coefficients. The existence of two different regimes in the stirred cell was characterized respectively by the presence of a boundary layer at the interface at low stirring speeds ($\leq$100 rpm) and by surface renewal at high stirring speeds ($\geq$200 rpm). Therefore, the mass transfer coefficient for the base, k_B, is related to the

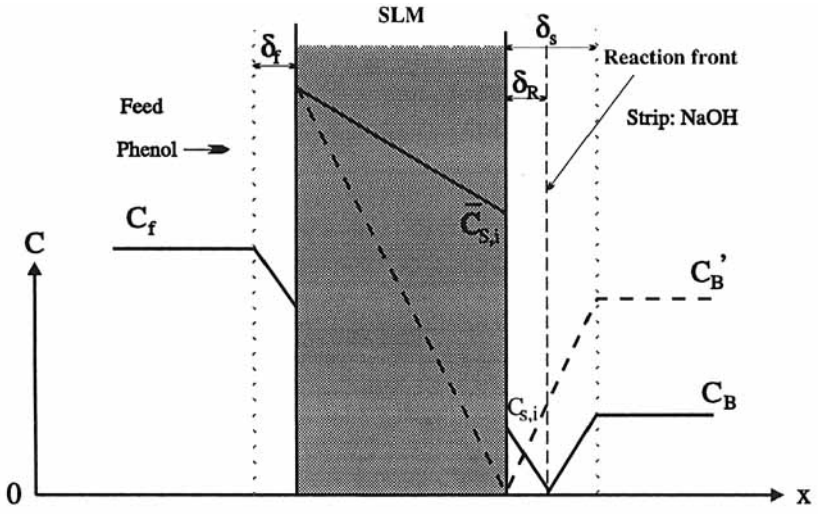

FIG. 1 Concentration profiles for facilitated transport of phenol through an SLM with insufficient base in strip.

phenol transfer coefficient k_s in the strip as

$$k_B = k_S D_B / D_A \tag{7}$$

according to the film theory, which was also used by Basu et al. (12), and as

$$k_B = k_S (D_B / D_A)^{1/2} \tag{8}$$

according to the surface renewal theory.

The mass transfer rate can then be correlated with the total mass transfer coefficient in Eq. (2) through the following equation:

$$J_A = K\left(C_f + \frac{m_s D_B}{q m_f D_A} C_B\right) \tag{9}$$

Phenol Transport through Partly Decayed SLMs

Loss of membrane liquid to the adjacent aqueous solutions is a frequent observation in the operation of SLMs. It is assumed here that either the feed or strip solution penetrates the membrane pores after loss of the membrane liquid. This assumption has been verified experimentally by a study using impedance spectroscopy (13). The exact solution of the effect of membrane liquid loss on the mass transfer rate should take into account the distribution of the phase interface within the decayed membrane pores

(i.e., membrane liquid preferentially lost from larger pores) and integrate all the infinitesimal elements. However, it is impossible to obtain the exact solution because of uncertainty about the location of the decayed interface. Therefore, it is assumed that the loss of solvent is the same over the whole membrane area, and the aqueous layer within the SLM can be represented by a certain thickness. Although this assumption presumably deviates from reality, the results can provide a qualitative guide to the effect of membrane liquid loss on the mass transfer rate and even indicate whether feed or strip actually penetrates the membrane pores. Two cases are considered below.

(1) The feed solution penetrates the membrane pores. The thickness of the aqueous layer within the membrane pores is δ_{mf}, as shown schematically in Fig. 2. The membrane resistance to phenol transport is the sum of the resistances of the aqueous layer (δ_{mf}) and the organic layer ($\delta_m - \delta_{mf}$),

$$R_m = \frac{1}{k_{mf}} + \frac{1}{m_f k'_m} \tag{10}$$

$$= \frac{\tau}{\epsilon}\left(\frac{\delta_{mf}}{D_A} + \frac{\delta_m - \delta_{mf}}{m_f D_{Ao}}\right)$$

The derivative of R_m with respect to the thickness δ_{mf} of the aqueous layer is

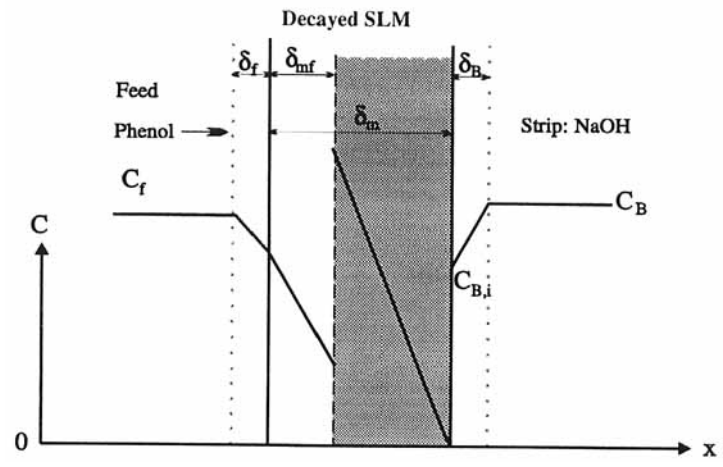

FIG. 2 Concentration profiles for facilitated transport of phenol through a partly decayed SLM.

$$\frac{dR_m}{d\delta_{mf}} = \frac{\tau}{\epsilon}\left(\frac{1}{D_A} - \frac{1}{m_f D_{Ao}}\right) \tag{11}$$

If $dR_m/d\delta_{mf} > 0$, the membrane resistance increases as the feed penetrates the membrane pores and the phenol transfer rate will decrease. Otherwise the penetration of the feed solution into the pores increases the mass transfer rate. The effect depends on the relative magnitudes of D_A and $m_f D_{Ao}$.

(2) The SLM is partly invaded by the stripping solution and the thickness of the aqueous layer is δ_{ms} (Fig. 3). The chemical reaction front may be at the phase interface or somewhere in the film of the aqueous solution depending on the concentration of base. Similar to Eq. (6), the critical base concentration can be expressed as

$$C'_B = qK'C_f/k'_B \tag{12}$$

The dotted lines in Fig. 3 represent the concentration profiles at the critical concentration. Here K' is the mass transfer coefficient through the feed and the organic phase, and it can be related to the individual transfer coefficients by the relation

$$\frac{1}{K'} = \frac{1}{k_f} + \frac{1}{m_f k''_m} = \frac{1}{k_f} + \frac{(\delta_m - \delta_{ms})\tau}{m_f D_{Ao}\epsilon} \tag{13}$$

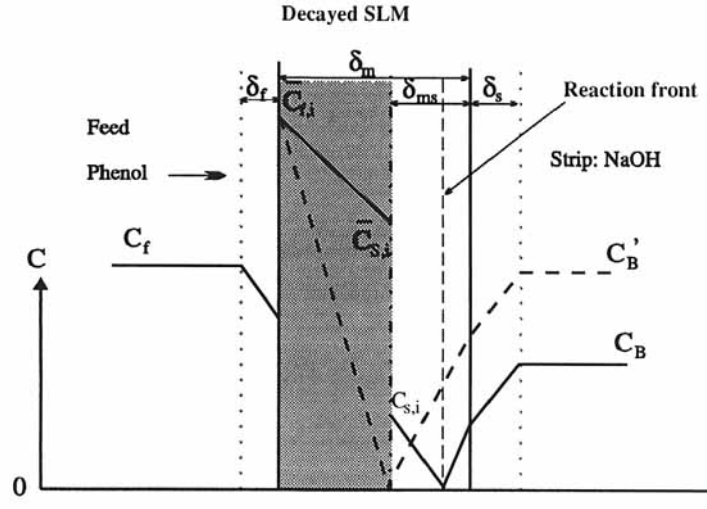

FIG. 3 Concentration profiles for facilitated transport of phenol through a partly decayed SLM with insufficient caustic in strip.

The term $1/k'_B$ in Eq. (12) is the sum of the resistances for transfer of the base in the strip and in the aqueous layer within the membrane, and equals

$$\frac{1}{k'_B} = \frac{1}{k_B} + \frac{\delta_{ms}\tau}{D_B\epsilon} \tag{14}$$

If the mass transfer coefficient for the base, k_B, is not available, it can be related to k_s through Eq. (7) according to the film theory, or Eq. (8) according to the surface renewal theory. From Eqs. (12)–(14) it can be seen that as the thickness of the aqueous layer in the membrane, δ_{ms}, increases, the critical base concentration also increases. This means that, at a certain base concentration, the reaction front may move away from the phase interface into the aqueous phase and a deficient region forms within the membrane as the strip penetrates the membrane pores.

If the stripping base concentration is lower than the critical value given in Eq. (12), the phenol transfer rate is expressed by Eq. (9) and the total resistance can be obtained as

$$\frac{1}{K} = \frac{1}{k_f} + \frac{1}{m_f k''_m} + \frac{m_s}{m_f}\left(\frac{1}{k_{ms}} + \frac{1}{k_s}\right) \tag{15}$$

The membrane resistance is now

$$R_m = \frac{1}{m_f k''_m} + \frac{m_s}{m_f k_{ms}} \tag{16}$$

$$= \frac{\tau}{\epsilon}\left(\frac{\delta_m - \delta_{ms}}{m_f D_{Ao}} + \frac{m_s \delta_{ms}}{m_f D_A}\right)$$

The derivative of R_m with respect to the thickness of the aqueous layer δ_{ms} is

$$\frac{dR_m}{d\delta_{ms}} = \frac{\tau}{\epsilon}\left(\frac{m_s}{m_f D_A} - \frac{1}{m_f D_{Ao}}\right) \tag{17}$$

If the stripping base concentration is equal to or higher than the critical value, the mass transfer rate is given by Eq. (4) and the total resistance is reduced to

$$\frac{1}{K} = \frac{1}{k_f} + \frac{(\delta_m - \delta_{ms})\tau}{m_f D_{Ao}\epsilon} \tag{18}$$

In this case, the total mass transfer resistance decreases with the penetration of the stripping phase into the membrane pores (i.e., as δ_{ms} increases).

EXPERIMENTAL

Chemicals and Membranes

Loose crystal phenol, sodium hydroxide pellets, and sodium nitrate used for the preparation of aqueous solutions were obtained from Ajax Chemicals and were of analytical grade. The membrane liquids, anhydrous *n*-decanol, *n*-dodecane, Span 80 (sorbitan monooleate), and Tween 80 (polyethylene sorbitan monooleate), are products of Sigma. Kerosene was purchased from Aldrich for laboratory use. All the chemicals were used without further purification.

Celgard (Hoechst Celanese), Durapore (Millipore), and Anopore (Whatman) membranes were used in the experiments. The physical parameters of these membranes are listed in Table 1. The data were obtained from the manufacturer's specifications except where indicated. The SLMs were prepared by immersing the support membrane in the membrane liquid for more than 1 hour to ensure complete wetting of all membrane pores.

Determination of Phenol Distribution Coefficient

Distribution coefficients of polar organic solvents for phenol are usually much higher than those of nonpolar organic solvents, but unfortunately, polar organic solvents have much higher solubility in water and lower interfacial tension at the same time. Methyl isobutyl ketone (MIBK) has been used by a few researchers in the removal of phenol by membrane extraction and with SLMs (2, 8). However, because of its high solubility in water, MIBK was easily lost from membranes and an SLM with MIBK as its membrane liquid decayed even within 1 hour (7). In the present work, *n*-decanol was selected as the main membrane liquid. The theoreti-

TABLE 1
Characteristics of Membranes Used

Membrane	Material	Pore size (μm)	Thickness δ (μm)	Porosity ε (%)	Tortuosity τ
Celgard 2500	Polypropylene	0.075 × 0.25	25 ± 2.5	45	2.25[a]
Anopore 0.2	Anodized alumina	0.20	73.0 ± 6.6[b]	66.3[b]	1
Durapore GVHP	PVDF	0.22	110 ± 7[c]	75	1.67[d]

[a] Reference 14.
[b] Reference 15.
[c] Measured with a micrometer from 10 pieces of membranes.
[d] Calculated using equation $\tau = (2 - \epsilon)/\epsilon$ (16).

cally estimated distribution coefficient of phenol in *n*-decanol is 27.4 (2), which is acceptable for the SLM process. However, the solubility of *n*-decanol in water is much lower than those for MIBK and *n*-butyl acetate. Mixtures of kerosene/Span 80 and kerosene/Tween 80 were also used as the membrane liquids to compare the effect of distribution coefficient on the phenol transfer rate.

Distribution coefficients for phenol between organic solvents and aqueous solutions were determined by conventional solvent extraction at 20°C. Phenol concentration in the aqueous phases before and after extraction was analyzed by UV spectroscopy (Shimadzu UV-120-02) at a wavelength of 272 nm. Phenol concentration in the organic phase was obtained by mass balance. In the case of *n*-decanol as a solvent, the effect of solubility on the phase volumes was considered in the calculation.

The rates of extracting phenol by mixtures of *n*-decanol and *n*-dodecane were determined to evaluate the possible resistance caused at the phase interface. Fifty milliliters each of the organic and the phenol aqueous solutions were fully mixed in an Erlenmeyer flask by magnetic stirring. Five milliliter samples were taken out at defined time intervals for analysis. The samples were immediately centrifuged to separate the two phases.

Measurements of Phenol Transport

Experiments for phenol removal by SLMs were carried out in the batch apparatus shown in Fig. 4. The membrane contacting area with an aqueous solution was 10.2 cm^2, and the effective volume of each chamber was measured by weighing as 74 mL. The stirring disk in each chamber was propelled by an adjustable 9-position stirrer (Cole-Palmer). Samples were taken from the feed sampling ports at regular intervals. The apparatus and the stirrer were placed in a constant temperature room and controlled at 20 ± 1°C. The mass transfer rate or flux was calculated from the slope of the concentration versus time curve as in Eq. (19):

$$J_A = -\frac{V}{A}\frac{dC_f}{dt} \tag{19}$$

where V is the volume of the feed solution and A is the membrane area contacting the feed solution.

Measurement of the Mass Transfer Coefficients

In order to evaluate the phenol transport through the SLMs, the phenol transfer coefficient in the bulk solution under stirring was measured. The apparatus used and the stirring condition were the same as in the flux

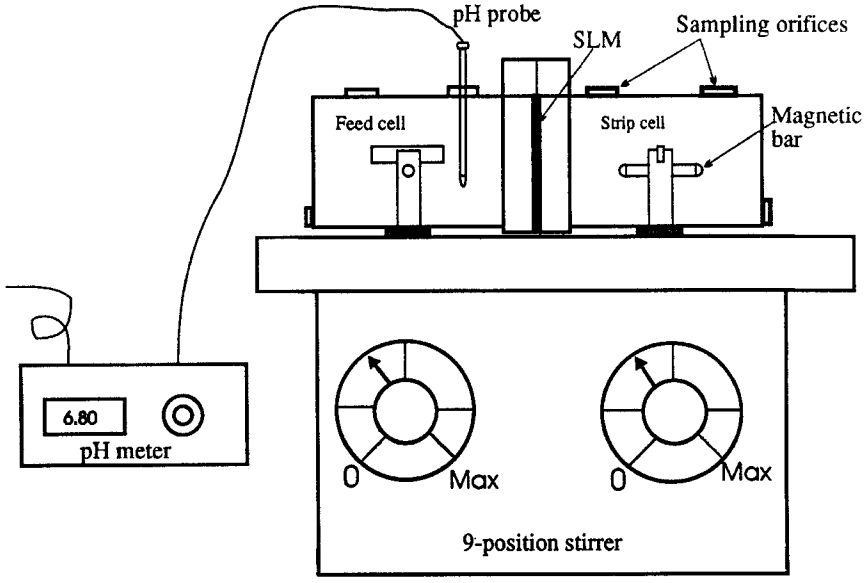

FIG. 4 Experimental setup.

measurement. Both chambers were filled with aqueous phenol solutions, but the concentration of phenol in one chamber (called the "receiving cell") was about 20% lower than in the other to allow effective diffusion to take place. The selected membrane was the Anopore anodized alumina membrane with a nominal pore size of 0.2 μm. This membrane is hydrophilic and wetted internally by aqueous solutions.

Phenol transported from the feed cell (higher concentration) through the membrane to the receiving cell. The difference in concentration between the two chambers was recorded periodically by sampling from the two cells and analyzing with the UV spectrophotometer. At steady-state conditions the concentration change in the two chambers versus time can be deduced through the integrated mass balance as

$$\ln \frac{\Delta C_0}{\Delta C} = \frac{2KA}{V} t \tag{20}$$

where $\Delta C_0 = (C_f - C_r)$ at time $t = 0$ and ΔC at time t. Values of the total mass transfer coefficient K can be obtained from the slope of a plot of $\ln (\Delta C_0/\Delta C)$ versus time t.

On the other hand, according to the resistance-in-series model the total transfer coefficient in the present system can be expressed as

$$\frac{1}{K} = \frac{1}{k_f} + \frac{1}{k_m} + \frac{1}{k_s} \tag{21}$$

Because the pore size of the Anopore 0.2 membrane is much greater than the diameter of the phenol molecule, the effect of the membrane pore wall on phenol diffusion can be neglected. Therefore, the intrinsic resistance of the membrane to phenol diffusion can be expressed as

$$1/k_m = \delta_m \tau/(D_A \epsilon) \tag{22}$$

In the present experiments, because the operating conditions were the same and the phenol concentrations were close in the two chambers, the resistances to phenol transfer in the two chambers were the same. Combining Eqs. (21) and (22), one obtains

$$\frac{1}{k_f} = \frac{1}{k_s} = \frac{1}{2}\left(\frac{1}{K} - \frac{\delta_m \tau}{D_A \epsilon}\right) \tag{23}$$

Therefore, by means of the measurement of the total mass transfer coefficient in the phenol diffusion process, the phenol transfer coefficient in the feed or strip chamber can be determined from Eq. (23).

RESULTS AND DISCUSSION

Some physical properties of *n*-decanol are listed in Table 2. The density was determined using a 5-mL pycnometer. The measurement of viscosity was carried out with a rotary viscometer (Haake VT 500). The diffusion coefficient of phenol in *n*-decanol was calculated according to the Wilke–Chang equation.

Results of Solvent Extraction

The phenol distribution coefficients were measured by conventional solvent extraction with an O/A volume ratio of 1 : 1. In the range of aqueous

TABLE 2
Physical Properties of *n*-Decanol at 20°C

Density (kg/m^3)	Viscosity (Pa·s)	D_{Ao} of phenol in decanol (m^2/s)	m of phenol between decanol–water	Solubility (wt%)[a]	
				Decanol in water	Water in decanol
830	13.58×10^{-3}	1.22×10^{-10}	20.6	0.0036	3.4

[a] Reference 17.

phenol concentrations from 0.05 to 2.5 g/L at equilibrium, the values of the distribution coefficient, m, remained essentially constant. The average value of m can be taken as 20.6.

The experiments for determining the rates of extraction of phenol were carried out under fast stirring conditions. This ensured full mixing of the phases, and only the interfacial resistance controlled the extraction process. The extraction rate for phenol was fast with n-decanol but much lower with n-dodecane. Figure 5 illustrates the percentage of phenol extracted versus time with two different mixtures of n-decanol and n-dodecane. When the organic mixture contained 40 vol% n-decanol, the extraction was nearly completed within 2 minutes, and it took a little longer if the initial aqueous phenol concentration was high. For extraction with 30 vol% n-decanol, the extraction rate was obviously slower. It took about 10 minutes for the completion of extraction when the initial phenol concentration was low. From these results it can be concluded that if the content of n-decanol in the mixtures of n-decanol/n-dodecane is higher than 40 vol%, the rate for extraction of phenol is fast and the interfacial resistance can be neglected. The interfacial resistance will become noticeable when the n-decanol content is lower than 30 vol%.

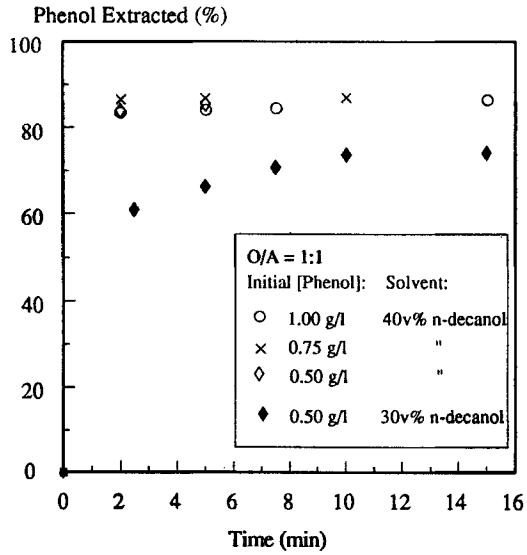

FIG. 5 Rate of phenol extraction with mixed n-decanol and n-dodecane.

Phenol Mass Transfer Coefficients in Stirred Chambers

The reliability of the method described above for measuring the mass transfer coefficients in the stirred chambers is largely dependent on the membrane used. Ideally, the membrane pores should be straight to give a tortuosity of 1. The only commercial membranes with straight pores are Anopore and Nuclepore membranes. However, it has been found that Nuclepore membrane pores deviate from cylindrical capillaries (18). Compared to Nucleopore membranes, the use of Anopore membranes offers several advantages. First, the membrane pores are straighter and well defined (15). Second, the membranes are less deformable because of the stiff alumina material. Also, the thickness and porosity of Anopore membranes are several times higher than those of Nucleopore membranes, which is favorable for measurement.

The resistance to phenol diffusion through the Anopore 0.2 μm membrane impregnated with water is calculated to be $1/k_m = 1.237 \times 10^5$ (s/m) using Eq. (22), and the data of membrane properties are given in Table 1. The diffusivity of phenol in water is calculated as $D_A = 8.9 \times 10^{-10}$ m²/s at 20°C using the Wilke–Chang equation.

Table 3 lists the overall mass transfer coefficient K of phenol diffusion at different initial concentrations as obtained experimentally according to the procedures described above. The corresponding phenol transfer coefficients in the stirred chambers were then calculated using Eq. (23), and they are also listed in Table 3. The error of K's obtained among experiments was less than 10%. It is noticed that the mass transfer coefficients decrease slightly with a decrease of phenol concentration. This could be due to experimental error. An average value of 11.8×10^{-6} m/s can be used for phenol concentrations up to 5.0 g/L.

In principle, the caustic transfer coefficient in the stirred chambers can also be determined by using the same method as for phenol. Unfortunately, the Anopore alumina membrane gradually dissolves in caustic solution, even if the concentration is as low as 0.1 mol/L. According to

TABLE 3
Mass Transfer Coefficients Measured for Phenol Diffusion

Initial phenol concentration (g/L)			
Feed cell	Receiving cell	K (10^{-6} m/s)	k_f or k_s (10^{-6} m/s)
5.0	4.4	3.60	12.97
1.0	0.80	3.41	11.81
0.20	0	3.22	10.68

Grosjean and Sawistowski (11), at a stirring speed of 330 rpm the surface renewal theory should apply. The mass transfer coefficient of the caustic in the chambers, k_B, can thus be estimated from Eq. (8) as 15.19×10^{-6} m/s. The diffusivity of NaOH in 0.10 mol/L aqueous solution was found to be 14.7×10^{-10} m^2/s (19).

Phenol Transport through SLMs

The standard conditions for phenol transport experiments was set as

Membrane liquid: *n*-decanol
Stripping solution: 0.10 M NaOH
Stirring speed: 330 rpm
Temperature: 20°C

(1) Phenol Removal in Different SLMs

Figure 6 shows how the ratios of phenol concentration in the feed cell over the initial value decreased with time in the liquid membrane supported by the Celgard 2500 membrane. Phenol could be removed efficiently from the aqueous solution. The profiles of C_f/C_{f0} change versus time were the same for the two different initial phenol concentrations,

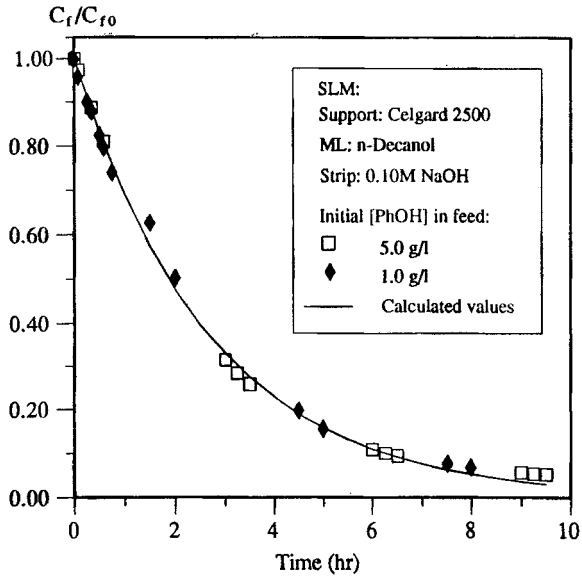

FIG. 6 Decrease of phenol concentration vs time for Celgard-SLM.

and 80% of phenol was removed in about 4 hours under the standard conditions. Figure 7 is a plot of C_f/C_{f0} versus time for the GVHP-SLM system. Compared to the Celgard 2500-SLM system, the phenol transfer was a little slower in this system and it took about 5 hours for the removal of 80% phenol.

Based on the measured distribution coefficient and mass transfer coefficient for phenol, the critical sodium hydroxide concentration in the strip can be calculated using Eq. (6). The critical strip concentration of NaOH is calculated to be 0.0260 M for the Celgard 2500-SLM and 0.0192 M for the GVHP-SLM systems at the initial phenol concentration of 5 g/L. Therefore, the use of 0.1 M NaOH as strip can assure the facilitated transport of phenol.

For the facilitated transport through an SLM, the phenol transfer rate can be described by Eqs. (4) and (5) when $C_B \geq C'_B$. The mass balance for the feed cell is

$$-V_f dC_f/dt = AKC_f \tag{24}$$

Integrating the above equation, one obtains

$$\frac{C_f}{C_{f0}} = \exp\left[-\left(\frac{AK}{V}\right)t\right] \tag{25}$$

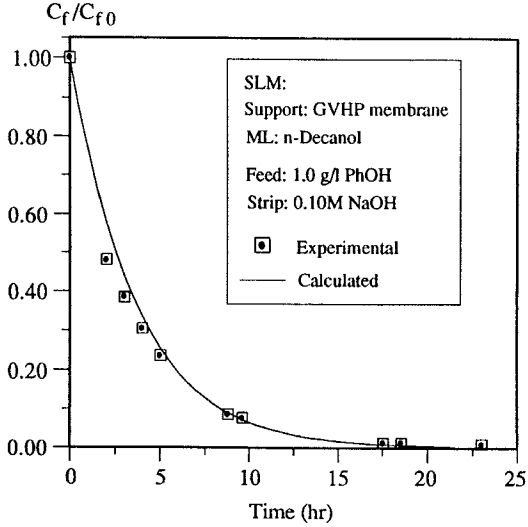

FIG. 7 Decrease of phenol concentration vs time for GVHP-SLM.

where C_{f0} and C_f represent the phenol concentrations at the initial time and any time t. The solid curves in Figs. 6 and 7 are calculated from Eqs. (5) and (25) using the separately determined values of k_f, m, and k_m. It can be seen that the estimated values are in very good agreement with the experimental results. This is evidence that the method proposed is reliable for measuring individual mass transfer coefficients in the stirred cell. It is noted that, in Figs. 6 and 7, at longer times the experimental results depart from the estimated ones, i.e., the mass transfer rate tends to be lower than expected, especially in the case of the Celgard-SLM (Fig. 6). This discrepancy might be due to the gradual loss of membrane liquid which is not accounted for in Eq. (25) and will be discussed in detail later.

The organic solvents with a low distribution coefficient for phenol were also tested as the membrane liquid. Two mixed solvents were selected: 5 vol% Span 80 in kerosene and 5 vol% Tween 80 in kerosene. The former mixture easily forms water-in-oil (W/O) emulsions, and the latter forms oil-in-water (O/W) emulsions. The distribution coefficient for phenol between 5% Span in kerosene and water was reported as only 1.0 (6). A similar value can be expected for the 5% Tween in kerosene as the solvent. Figure 8 shows the decrease of phenol concentration with time for the

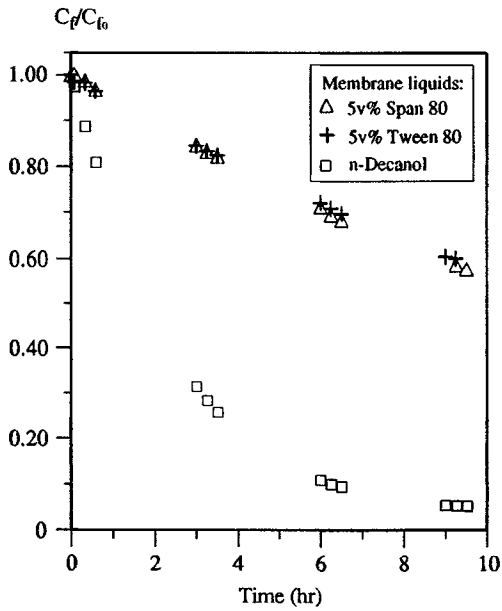

FIG. 8 Removal of phenol by SLMs using different solvents.

Celgard-SLM. The theoretical calculation was not carried out because of the lack of phenol diffusivities in the organic mixtures. About 40% phenol was removed in 8 hours. Compared to the results in Fig. 6, phenol removal was much slower using kerosene-based solvents. This indicates that the membrane liquid used in SLMs plays an important role in phenol removal. Both high distribution coefficient and good stability are required in the selection of membrane liquids.

(2) Effect of Feed Phenol Concentration

Phenol mass transfer rates or phenol fluxes were calculated according to Eq. (19) from the measurement of phenol concentration change with time. The standard conditions were used in this case. It was observed that the initial fluxes obtained for different feed phenol concentrations were consistent with the fluxes determined over a single experiment with a gradual change of C_f. The effect of feed phenol concentration on the flux is illustrated in Fig. 9. In the concentration range up to 5 g/L, the flux was observed to be linearly proportional to the feed phenol concentration, which agrees with the theoretical analysis. The solid line in Fig. 9 represents Eq. (4), which is close to the experimental results.

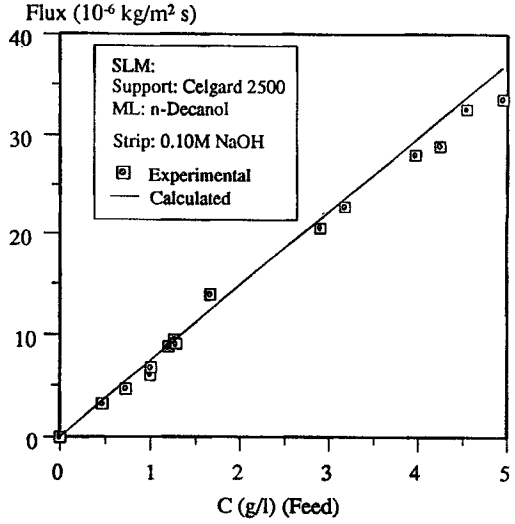

FIG. 9 Phenol flux vs feed concentration.

(3) Effect of Salt Concentration on Phenol Flux

Industrial phenolic wastewater often contains salts. The presence of salt affects the properties of the aqueous solutions, such as phenol diffusivity, viscosity, and density. In SLMs, the total combined effect of salt concentration is reflected in the mass transfer coefficients. Experiments were conducted to investigate the possible effect of the presence of salt on the flux of phenol. The feed and/or strip solutions used in these experiments were prepared by adding certain amounts of sodium nitrate salt to the aqueous solutions. Sodium nitrate was chosen because of its high solubility in water. Under the standard conditions, fluxes were measured. Figure 10 is a comparison of phenol fluxes with and without salt. Under the same operating conditions with the Celgard-SLM, adding salt to the feed or strip solutions up to 6 mol/L had no obvious effect on the phenol flux. It can be concluded that the presence of salt in the aqueous solutions has essentially no effect on the phenol transport through SLMs. However, the presence of salt can play an important role in the stability of SLMs (20, 21).

(4) Effect of Stirring Speed on Phenol Flux

The effect of stirring speed in the feed and strip chambers was investigated. Figure 11 is a plot of the experimental results. In the range from

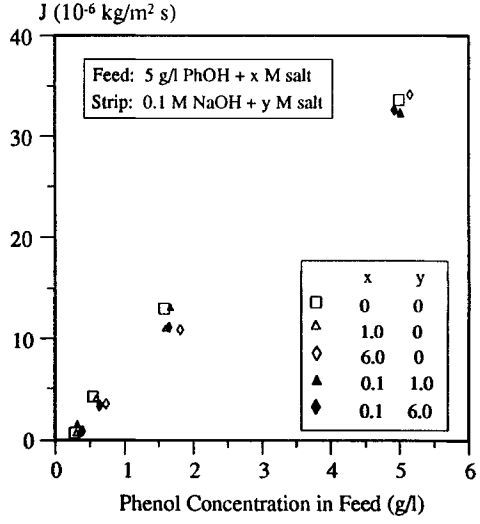

FIG. 10 Effect of $NaNO_3$ concentration on phenol flux.

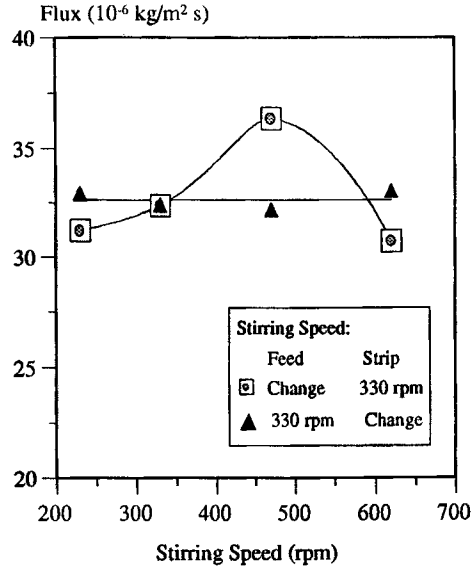

FIG. 11 Phenol flux through Celgard-SLM vs stirring speed.

230 to 620 rpm, variation of stirring speed in the strip cell had no effect on the phenol flux. However, increase in stirring speed in the feed cell increased the phenol flux to a maximum, and then further increase caused a decrease in flux.

At the highest stirring speed of 620 rpm, some small oil droplets could be visibly observed in the feed chamber. Under the operating conditions, the stripping caustic concentration (0.1 M) exceeded the critical value given by Eq. (6), and the phenol transfer rate is described by Eqs. (4) and (5). It can be seen that phenol flux is independent of stirring speed in the strip side, which is consistent with the experimental results. At higher stirring speed in the feed chamber, the resistance to phenol transfer in the feed side decreases and phenol flux should increase. This is reflected in Fig. 11 when the stirring speed in the feed cell was changed from 230 to ~500 rpm. The phenol flux decline at a speed higher than 500 rpm could be caused by the serious loss of membrane liquid to the feed solution. A visual observation partly confirmed this presumption. That loss of membrane liquid at the feed side causes a decline of phenol flux will be discussed later. Little influence of high stirring speed in the stripping chamber on phenol flux indirectly suggests that the membrane liquid loss was insensitive to the conditions in the stripping chamber and mainly caused through the feed chamber. This is consistent with the mechanism of membrane

liquid loss proposed elsewhere (20) and has been confirmed by impedance spectroscopy (13).

(5) Phenol Flux Decline with Time

It was observed in Figs. 6 and 7 that the phenol transfer rate was slower than theoretically expected as the operating time extended. This phenomenon was further investigated by measuring the phenol flux change over a long time. The phenol flux was measured every day until a sudden increase in feed pH value or the pH value in the feed became close to that in the strip, indicating that direct channeling occurred between feed and strip solutions and the SLM had failed. When a measurement of flux was to be conducted, the feed and strip solutions were drained out but the SLM was left intact. Both chambers were rinsed twice with the respective fresh solutions. The two chambers were then filled with the respective fresh solutions and followed by immediate start of stirring and measuring the concentration change with time. If no membrane liquid loss had occurred, the flux should have remained nearly the same because the operating conditions and the solutions were the same for each measurement of flux. However, flux decline with time was observed for both Celgard 2500 and GVHP supported liquid membranes, as shown in Figs. 12 and 13.

Figure 12 is the time course for the flux decline versus time in the

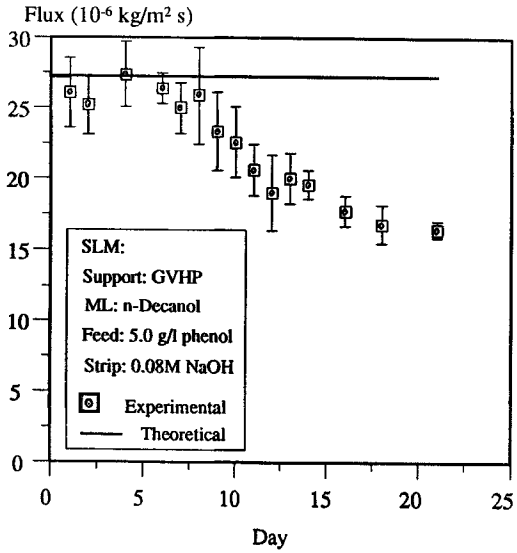

FIG. 12 Phenol flux decline vs time for GVHP-SLM.

GVHP-SLM. Over the first 8 days, phenol flux fluctuated a little around 27×10^{-6} kg/m^2·s. From Day 9, an obvious flux decline occurred and the decrease of flux continued till Day 21. On Day 22, a noticeable leakage between the two cells was detected and the bridging of the feed and strip solutions took place. The SLM was considered as terminated with a lifetime of 21 days. Figure 13 is a plot of phenol flux change versus time for the Celgard 2500-SLM. The flux began decreasing on the second day and the lifetime was only about 73 hours (~3 days). One of the causes for the much shorter lifetime of the Celgard-SLM could be due to its smaller thickness, which was only ~1/4 of that for the GVHP membrane.

The solid lines in Figs. 12 and 13 represent the theoretical fluxes based on Eqs. (4) and (5). If the SLMs had not degraded, the flux should have remained the same level as the theoretical estimation. The phenomena of the flux decline and membrane leakage can be attributed to the loss of membrane liquid to the adjacent aqueous solutions because of the SLM instability.

(6) Estimation of Membrane Liquid Loss Based on the Theoretical Analysis

On the basis of the theoretical analysis, it is possible to estimate which of the aqueous solutions (feed or strip) is the most probable to penetrate

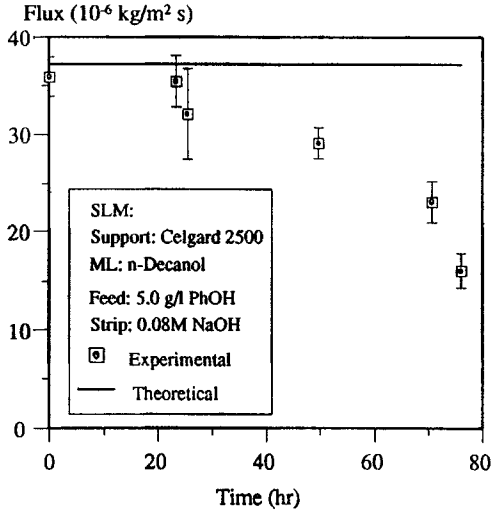

FIG. 13 Phenol flux decline vs time for Celgard 2500-SLM.

the pores after the loss of membrane liquid. If the decayed SLM is penetrated by the feed solution, the changed membrane resistance to the phenol transport is expressed by Eq. (10). From Eq. (11) it can be calculated that $dR_m/d\delta_{mf} > 0$ for phenol transport through a membrane impregnated with *n*-decanol. This means that penetration of feed solution into the SLM increased the mass transfer resistance and caused the decrease of phenol flux.

However, if it was the feed solution only that penetrated the SLMs, two aspects of the experimental results cannot be explained. First, according to Eqs. (4), (5), and (10), it can be calculated that even if 99% of the membrane liquid was lost and replaced with the feed solution, the flux would only decrease to ~60% of its initial value. But the experimental results show that phenol flux through the Celgard 2500-SLM decreased to the 45% level before leakage. Second, if the loss of membrane liquid was a gradual process, the flux should have decreased gradually from the beginning according to the feed penetration assumption. However, the flux remained essentially unchanged for the first few days in the GVHP-SLM. In summary, the flux decay phenomenon may be partly caused by penetration of the feed solution into the SLM. However, it is likely that there are additional factors that contribute to the flux decay in SLMs.

If the SLM decays and is refilled with the strip solution, at a certain base concentration the reaction front moves away from the phase interface into the film of the aqueous phase in the membrane and a deficient region forms. Using Eqs. (12)–(14), corresponding to a stripping base concentration, one can calculate the critical aqueous layer thickness δ'_{ms} within a membrane at which a deficient region begins to form. For the Celgard 2500-SLM under the experimental conditions and with a caustic concentration of 0.10 mol/L as the strip, $\delta'_{ms} = 21$ μm, which is about 4/5 of the membrane thickness. This means that when the strip solution penetrates ~4/5 depth of membrane capillaries, the deficient region will begin to form. For the GVHP-SLM, $\delta'_{ms} = 0.665$ μm, which is 2/3 of the membrane thickness. Therefore, the penetration of strip solution into the membrane may cause the formation of a deficient region, and once this occurs the mass transfer resistance may increase quickly as the reaction front moves away from the phase interface into the aqueous film.

If the base concentration is higher than the critical one, the penetration of strip solution into the SLM can decrease the mass transfer resistance and increase the phenol flux according to Eq. (18). However, if the base concentration is lower than the critical value, the mass transfer resistance increases greatly. From Eq. (17) it can be calculated that $dR_m/d\delta_{ms} > 0$. This means that penetration of the strip solution into the SLM (thus increasing the aqueous layer thickness within the membrane) increases the

mass transfer resistance (Eqs. 15 and 16) if the strip base concentration is lower than the critical value.

Under the present experimental conditions, the caustic concentration in the strip (0.10 mol/L) exceeded the initial critical values for both the Celgard-SLM and the GVHP-SLM. However, if ML is lost and the stripping solution penetrates into the membrane pores, the stripping caustic concentration could became lower than the critical values. Take the GVHP-SLM as an example. It was estimated above that the critical aqueous layer thickness $\delta'_{ms} = 0.665$ μm, and this thickness corresponds to a critical caustic concentration $C'_B = 0.10$ mol/L. If the stripping solution penetrated further into the membrane pores, the stripping caustic concentration (0.10 mol/L) would be lower than the critical value, and therefore a deficient region would form.

The above analysis of the decayed SLMs is based on the assumption that the decayed region within the membrane is uniformly distributed. The actual decayed interface could be a complicated shape, and up to now there is no method that can be used to locate this phase interface. However, the analysis can offer a qualitative guide to the effect of membrane liquid loss on the flux. For example, with the penetration of the stripping solution into the membrane pores, a deficient region may not form over the whole membrane area, but it is possible that deficient regions form in some pore channels, especially in large pores. In this case, mass transfer resistance to phenol would increase with penetration of the stripping solution into parts of the membrane.

Some authors have mentioned the possible presence of an interfacial resistance in mass transfer with instantaneous chemical reactions, and the interfacial resistance was attributed to the presence of ionic salts (11). It is not known whether an interfacial resistance exists at the reaction front of the strip side in the present system, where sodium hydroxide reacts with phenol to form phenolate. However, when the strip solution penetrates into membrane pores, it may be more difficult for the phenolate salt formed to diffuse away from the reaction front into the bulk strip solution. If this is true, the formation of a deficient region at the strip side would occur more easily and the δ'_{ms} could be less than estimated above.

CONCLUSIONS

SLMs are feasible for the removal and recovery of phenol from waste effluents. The key to this technology relies on the selection of a suitable SLM. The physical properties of the membrane liquid and the support have great influence on the phenol flux and the lifetime of the process.

In this study, *n*-decanol was chosen as a membrane liquid for the phenol removal. Compared to kerosene-based solvents or MIBK as membrane liquid, a higher phenol flux with the *n*-decanol impregnated SLM has been obtained than with the former, and a longer lifetime achieved than with the latter. Phenol flux increased with feed phenol concentration, passed through a maximum with stirring speed, and was not influenced by the presence of salt ($NaNO_3$).

The lifetime of the SLM varied with the membrane support. A thicker membrane, as in the case of the GVHP membrane, tends to have longer lifetime than a thinner membrane, e.g., Celgard 2500. However, the increase in membrane thickness increases the mass transfer resistance and lowers the initial flux. Under the experimental conditions, the lifetime of the GVHP-SLM was 21 days but that of the Celgard 2500-SLM was only about 3 days. It should be noted that the GVHP and Celgard membranes are not necessarily optimal. As reported elsewhere (22), membranes with a morphology having a less connected network and sharp pore edges can be anticipated to have longer lifetimes than those obtained in the present experiments.

The phenol transfer process through SLMs can be quantitatively estimated according to models based on the resistance-in-series method. A significant conclusion is that the models developed for the decayed SLMs provide an insight into the effect of membrane liquid loss and penetration of aqueous solutions on the phenol flux.

An experimental method is proposed for the measurement of mass transfer coefficients in the bulk phases by employing the well-characterized Anopore membrane. The method is especially useful in the case of a permeation apparatus where the estimation of individual mass transfer coefficients is difficult.

NOMENCLATURE

C	concentration (g/L, mol/L)
C'	critical concentration (g/L, mol/L)
$\overline{C}$	concentration in organic membrane phase (g/L, mol/L)
D	diffusivity (m^2/s)
J	mass transfer rate or flux ($kg/m^2 \cdot s$)
k	individual mass transfer coefficient (m/s)
K	overall mass transfer coefficient (m/s)
m	distribution coefficient, $m = C_{org}/C_{aq}$ (g/L)/(g/L)
q	stoichiometric coefficient (—)
R	mass transfer resistance (s/m)

Greek Letters

δ	thickness (m)
ϵ	membrane porosity (%)
τ	membrane tortuosity (—)

Subscripts

A	phenol solute
B	base
f	feed phase
i	interface
m	membrane
o	organic phase
R	reaction front
s	strip phase

ACKNOWLEDGMENT

The Australian Research Council is gratefully acknowledged for supporting this study.

REFERENCES

1. D. C. Greminger, G. P. Burns, S. Lynn, D. N. Hanson, and C. J. King, *Ind. Eng. Chem., Process Des. Dev.*, *21*, 51 (1982).
2. D. O. Cooney and C. L. Jin, *Chem. Eng. Commun.*, *37*, 173 (1985).
3. H. H. P. Fang and E. S. K. Chian, *Environ. Sci. Technol.*, *10*(4), 364 (1976).
4. G. L. Amy, B. C. Alleman, and C. B. Cluff, *J. Environ. Eng.*, *116*, 200 (1990).
5. R. Rautenbach and S. Klatt, in *Proceedings of Fifth International Conference on Pervaporation Processes in the Chemical Industry*, Heidelberg, Germany, March 11–15, 1991 (R. Bakish, Ed.), pp. 392–408.
6. T. Kataoka, T. Nishiki, and S. Kimura, *J. Membr. Sci.*, *41*, 197 (1989).
7. A. M. Urtiaga, M. I. Ortiz, and A. Irabien, *Inst. Chem. Eng. Symp. Ser.*, *119*, 35 (1990).
8. A. M. Urtiaga, M. I. Ortiz, E. Salazar, and J. A. Irabien, *Ind. Eng. Chem. Res.*, *31*, 877 (1992).
9. A. M. Urtiaga, M. I. Ortiz, E. Salazar, and J. A. Irabien, *Ibid.*, *31*, 1745 (1992).
10. A. Garea, A. M. Urtiaga, M. I. Ortiz, A. I. Alonso, and J. A. Irabien, *Chem. Eng. Commun.*, *120*, 85 (1993).
11. P. R. L. Grosjean and H. Sawistowski, *Trans. Inst. Chem. Eng.*, *58*, 59 (1980).
12. R. Basu, R. Prasad, and K. K. Sirkar, *AIChE J.*, *36*(3), 450 (1990).
13. F. F. Zha, A. G. Fane, H. G. L. Coster, and C. J. D. Fell, in *Proceedings of the 1993 International Congress on Membranes and Membrane Processes*, Heidelberg, Germany, August 30–September 3, 1993, p. 8.20.
14. J. R. Wolf and W. Strieder, *J. Membr. Sci.*, *49*, 103 (1990).

15. P. H. Hodgson, Ph.D. Thesis, The University of New South Wales, 1993, Chapter 2.
16. J. MacKie and P. Meares, *Proc. R. Soc. London, Ser. A, 232*, 498 (1955).
17. A. S. Kertes, *Solubility Data Series*, Vol. 15, Pergamon, New York, 1984, pp. 402–403.
18. A. Hernandez and F. Martinez-Villa, *Sep. Sci. Technol., 21*, 665 (1987).
19. E. W. Washburn (Ed.), *International Critical Tables of Numerical Data, Physics, Chemistry and Technology*, Vol. V, McGraw-Hill, New York, 1929, p. 67.
20. F. F. Zha, Ph.D. Thesis, The University of New South Wales, Australia, 1993.
21. A. M. Neplenbroek, D. Bargeman, and C. A. Smolders, *J. Membr. Sci., 67*(2&3), 133 (1992).
22. F. F. Zha, A. G. Fane, C. J. D. Fell, and R. W. Schofield, *Ibid., 75*, 69 (1992).

Received by editor February 14, 1994